Synthesis, characterization and photocatalytic performance of Au-ZnO nanopyramids

Electronic Supplementary Information

Oshadha K. Ranasingha,[a,b] Congjun Wang,[b,c] Paul R. Ohodnicki, Jr.,[b] Jonathan W. Lekse,[b,c] James P. Lewis,[a,b] Christopher Matranga*[b]

[a] *Department of Physics and Astronomy, West Virginia University, Morgantown, WV 26506, United States.*
[b] *National Energy Technology Laboratory, U.S. Department of Energy, 626 Cochrans Mill Road, Pittsburgh, PA 15236, United States.*
[c] *URS Corporation, P.O. Box 618, South Park, PA 15129, United States.*

1. Fourier Transform Infrared spectra of pure ZnO and Au-ZnO before and after the O_2 plasma etching

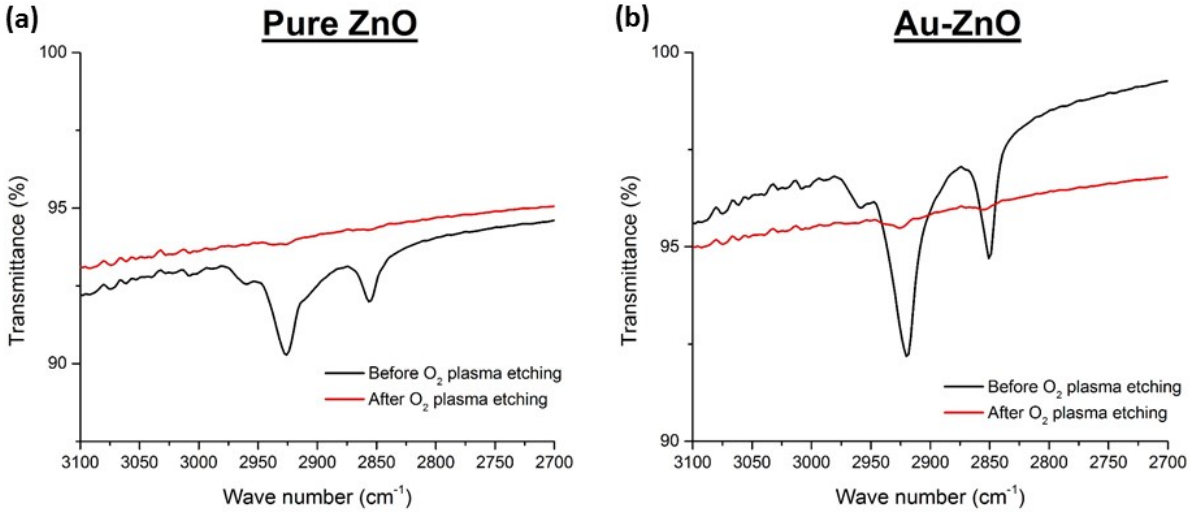

Fig. S1 (a) FTIR spectra of pure ZnO before (black) and after (red) the plasma etching (b) FTIR spectra of Au-ZnO before (black) and after (red) the plasma etching

2. Model calculation for plasmon resonance frequency red shift

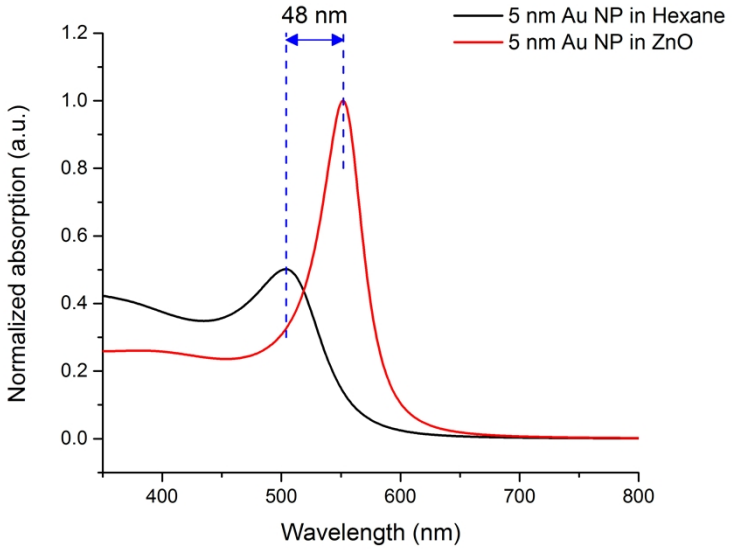

Fig. S2 Comparison of Au nanoparticle suspended in hexane and full embedded in ZnO

A model calculation was performed in order to support the experimentally observed red shift of the LSPR absorption peak. Our model calculations show that the LSPR peak occurs at 504 nm for a 5 nm Au nanoparticle suspended in hexane. When the Au nanoparticle is fully embedded in ZnO, LSPR peak can be found at 552 nm. The calculations was done according following an example shown in *Ohodnicki et al.*[1] The wavelength dependent dielectric constant of the Au was calculated according to *Etchegoin et al.*[2] The optical parameters (Table S1) were taken from previous reports.[2-4] The following equations give absorption cross section (Q_{abs}) and wavelength dependent dielectric constant($\in_{Au}(\lambda)$):

$$Q_{abs} = \frac{4\pi^2 a^3 \sqrt{\in_m}}{2\lambda} Im\left[\frac{\in_{Au} - \in_m}{\in_{Au} + 2\in_m}\right] \qquad \text{(Eq. S1)}$$

$$\in_{Au}(\lambda) = \epsilon_\infty - \frac{1}{\lambda_p^2\left(\frac{1}{\lambda^2} + \frac{i}{\gamma_p \lambda}\right)} + \sum_{j=1,2} \frac{A_j}{\lambda_j}\left[\frac{e^{i\phi_j}}{\left(\frac{1}{\lambda_j} - \frac{1}{\lambda} - \frac{i}{\gamma_j}\right)} + \frac{e^{-i\phi_j}}{\left(\frac{1}{\lambda_j} + \frac{1}{\lambda} + \frac{i}{\gamma_j}\right)}\right] \qquad \text{(Eq. S2)}$$

Where a is the radius of the nanoparticle, $\in_m$ is the dielectric constant of the matrix phase, λ is optical wavelength, ϵ_∞ is the high frequency limit dielectric constant, $\lambda_p$is the plasma wavelength, $\gamma_p$is the damping (expressed as a wavelength), λ_j is the interband transition wavelength, γ_j is the transition broadening (expressed as a wavelength), A_j is the dimensionless critical point amplitudes and ϕ_j is the phase which was fixed in to - $\pi/4$ according to the *Etchegoin et al.*[2]

Table S1. Optical parameters

Parameter	**Value**	**Source**
a	2.5 nm	Average radius from the TEM images
$\in_m$**(Hexane)**	1.88	*Mop*

		sik[4]
$\in_m$**(ZnO)**	3.70	*Azadetal.*[3]
ϵ_∞	1.53	*Etchegoinetal.*[2]
λ_p	145 nm	*Etchegoinetal.*[2]
γ_p	17000 nm	*Etch*

		e g o i n e t a l.[2]
λ_1	468 nm	*E t c h e g o i n e t a l.*[2]
λ_2	331 nm	*E t c h e g o i n e t a l.*[2]
γ_1	2300 nm	*E t c h e g o i*

		n e t a l.[2]
γ_2	940 nm	*E t c h e g o i n e t a l.*[2]
A_1	0.94	*E t c h e g o i n e t a l.*[2]
A_2	1.36	*E t c h e g o i n e t a*

		l.[2]
ϕ_1	- $\pi/4$ rad	*Etchegoinetal.*[2]
ϕ_2	- $\pi/4$ rad	*Etchegoinetal.*[2]

3. Tauc plots for direct band gap estimation

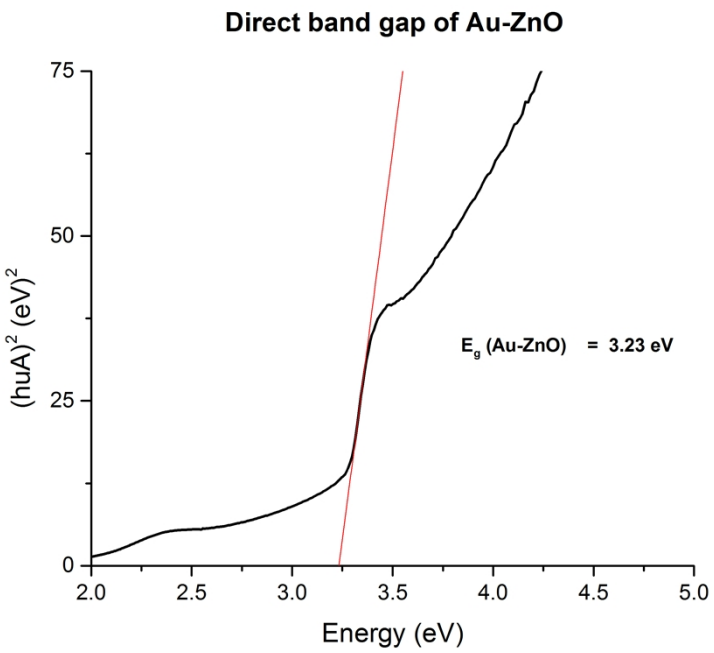

Fig. S3 Tauc plots for the direct band gap estimation of Au-ZnO.

4. TEM image of Au seeds

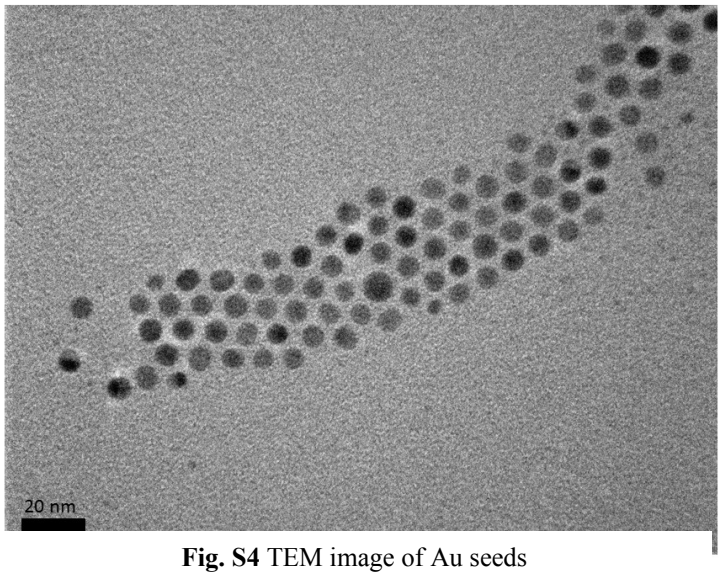

Fig. S4 TEM image of Au seeds

5. Au-ZnO interface analysis and HRTEM images of Au-ZnO

The HRTEM images of 9 Au/ZnO interfaces were analyzed using ImageJ software. A rectangular area in the middle of the ZnO nanoparticle consisting of 2.5 nm width and 4 lattice planes of length was chosen for the analysis. The average *d*-spacing of these 4 lattice planes was used as an estimate of the *d*-spacing of the corresponding rectangular area. Up to 20 lattice planes from the Au-ZnO interface were analyzed. The final results and error bars reported in the main text are the average values of all 9 Au-ZnO interfaces.

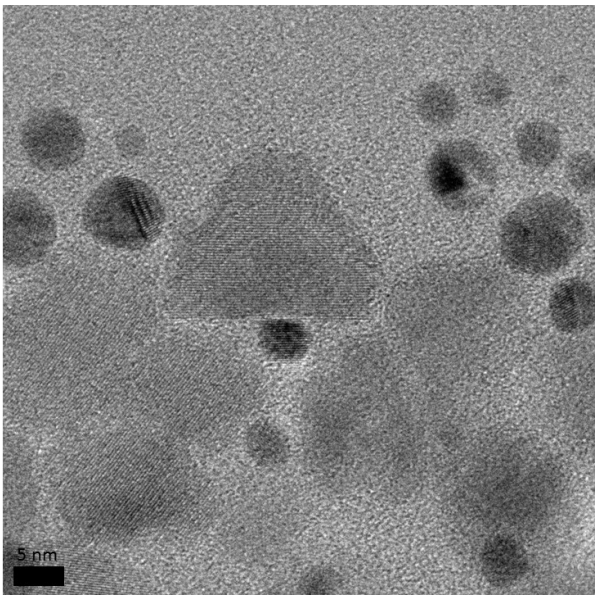

Fig. S6 Au-ZnO interface 1

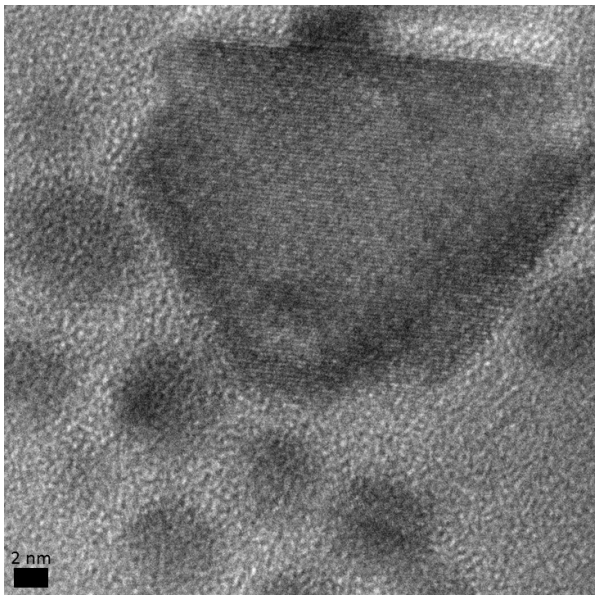

Fig. S7 Au-ZnO interface 2

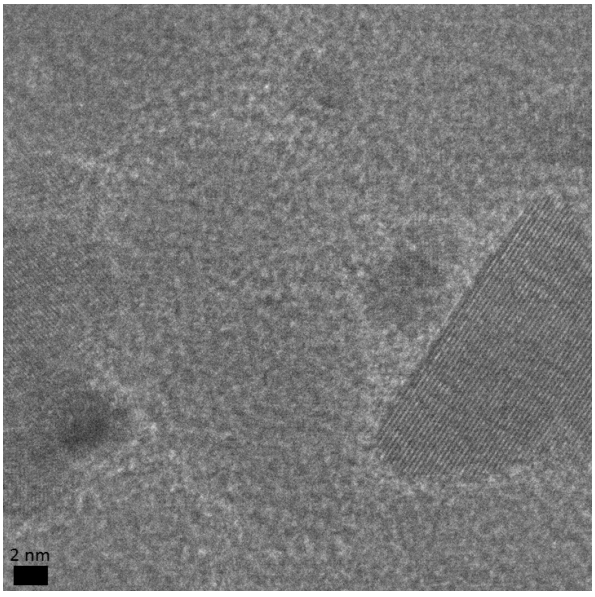

Fig. S8 Au-ZnO interface 3

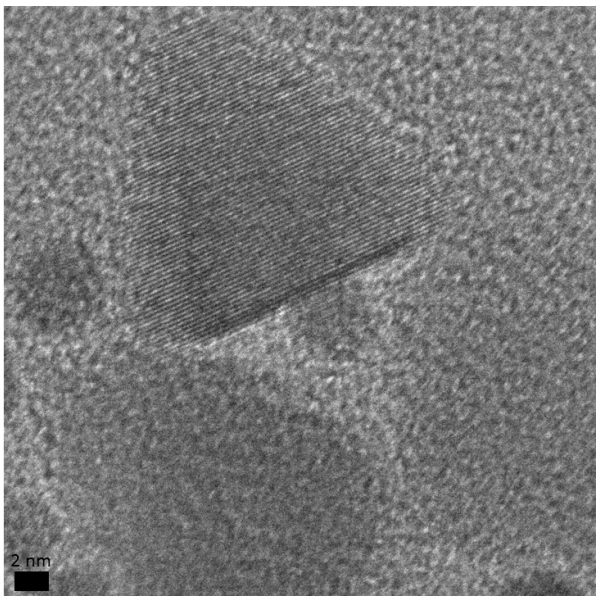

Fig. S9 Au-ZnO interface 4

6. Rietveld Analysis

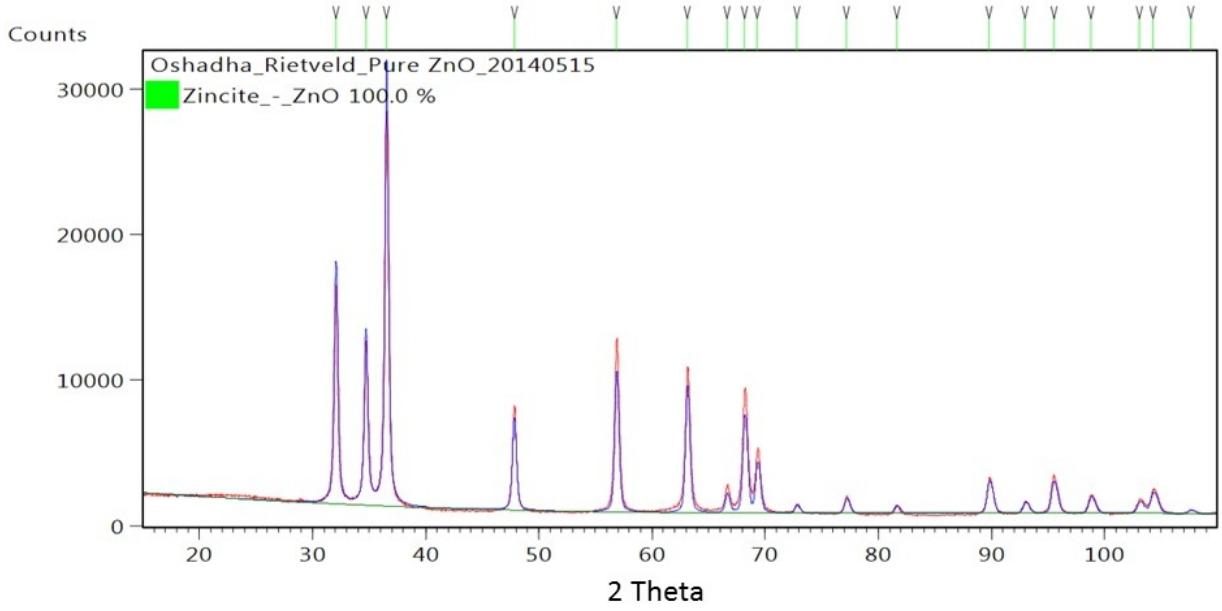

Fig. S10 High resolution XRD patterns with calculated pattern for pure ZnO

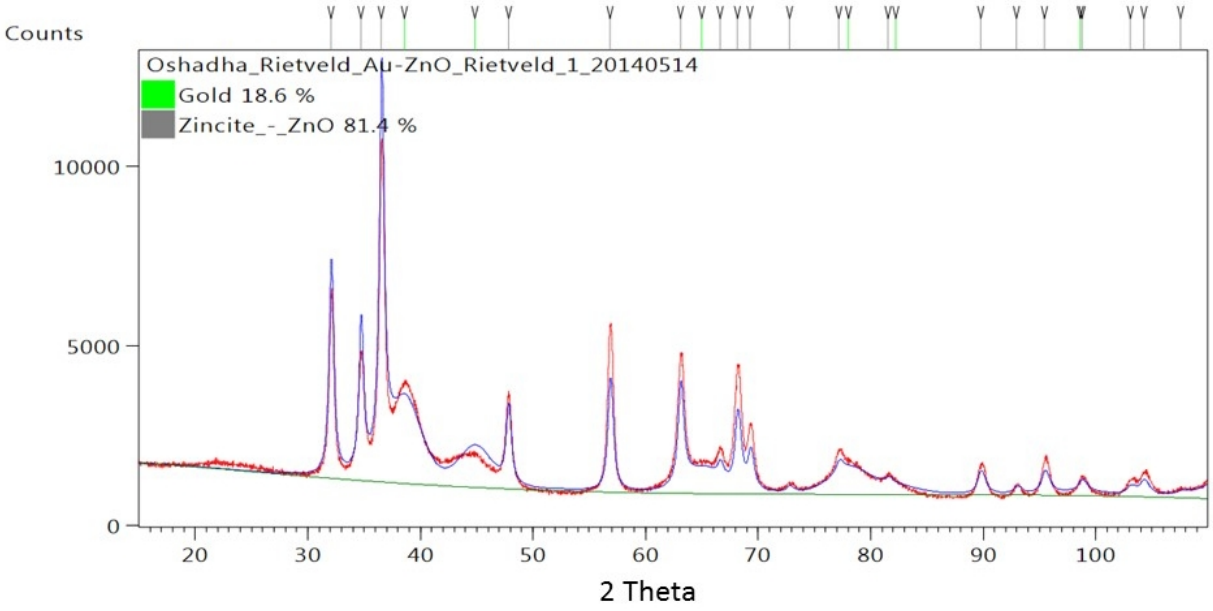

Fig. S11 High resolution XRD patterns with calculated pattern for Au-ZnO

7. Reaction kinetics of Au-ZnO for MB photodegradation

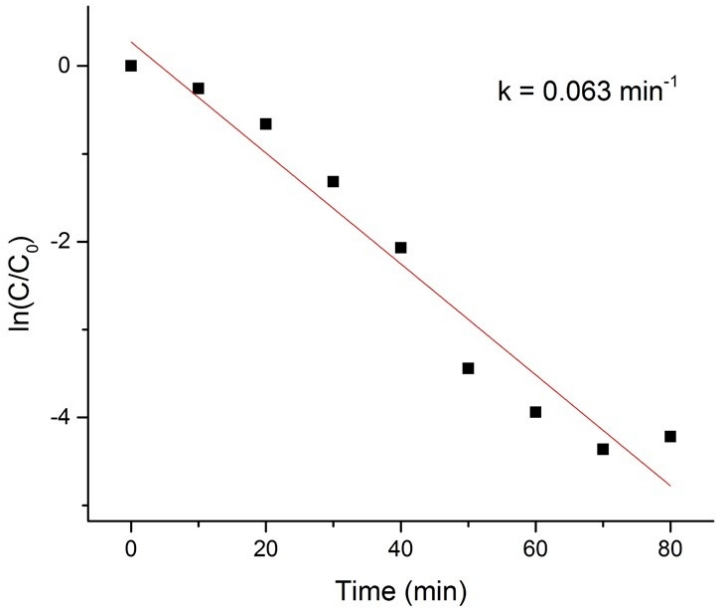

Fig. S12 Linear fit for ln(C/C_0) of MB versus time for Au-ZnO under $\lambda > 295$ nm illumination

ESI References:

1. P. R. Ohodnicki, M. P. Buric, T. D. Brown, C. Matranga, C. Wang, J. Baltrus and M. Andio, *Nanoscale*, 2013, **5**, 9030-9039.
2. P. G. Etchegoin, E. C. Le Ru and M. Meyer, *The Journal of Chemical Physics*, 2006, **125**, 164705.
3. A. K. Azad, J. Han and W. Zhang, *Applied Physics Letters*, 2006, **88**, 021103.
4. F. I. Mopsik *JOURNAL OF RESEARCH of the National Bureau of Standards - A. Physics and Chemistry* – 1967, **71A**, 287-292.